Inorganic Chemistry
Article

Inorg. Chem. **2011**, *50*, 1849–1855 **1849**
DOI: 10.1021/ic1022533

Tetradentate N_2S_2 Vanadyl(IV) Coordination Complexes: Synthesis, Characterization, and Reactivity Studies

Roxanne M. Jenkins, Tiffany A. Pinder, Michelle L. Hatley, Joseph H. Reibenspies, and Marcetta Y. Darensbourg*

Department of Chemistry, Texas A&M University, College Station, Texas 77843, United States

Received November 9, 2010

The versatile N_2S_2 tetradentate ligands $(bme\text{-}daco)^{2-}$, $(bme\text{-}dach)^{2-}$, and $(ema)^{4-}$ are known to accommodate many divalent transition-metal ions (M = Ni^{II}, Pd^{II}, Pt^{II}, Pb^{II}, Zn^{II}, Cd^{II}, Cu^{II}, and Fe^{II}) while maintaining reactivity at the *S*-thiolate sites of the respective N_2S_2M complexes. The vanadyl ion, of interest for its pharmacological possibilities and its spin-label reporter properties for bioinorganic studies, also shows an affinity for such mixed nitrogen/sulfur-donor environments. Thus, $(V{\equiv}O)^{2+}$ analogues of a well-characterized series of N_2S_2Ni complexes have been prepared as mimics of possible $N_2S_2(V{\equiv}O)$ formed from in vivo binding sites of the tripeptide motif, Cys−X−Cys. The nucleophilicity of the *S*-thiolate in these systems is explored with alkylating agents. IR [ν(VO)], electronic spectral, and electron paramagnetic resonance measurements are presented. X-ray diffraction studies of (bme-daco)(V≡O), (bme-dach)(V≡O), and $[Et_4N]_2[(ema)(V{\equiv}O)]$ further characterize the vanadyl complexes. A comparison of the spectral properties with the product of vanadyl interaction with the CGC tripeptide, the biological analogue of the tetraanionic N_2S_2 ligand, is given.

Introduction

The oxovanadium(IV) or vanadyl ion, $(V{\equiv}O)^{2+}$, is valued in metalloenzyme studies for its ability to replace divalent transition-metal ions that reside in both hard and soft ligand-donor sites and, in so doing, confer the electron paramagnetic resonance (EPR) reporter ability of the V^{4+} d^1 electronic configuration on that active site.[1,2] In addition, vanadium is itself of interest because the in vivo inhibition properties of the phosphotyrosine phosphatase enzyme have led to investigation of the vanadyl complexes [throughout the manuscript, the vanadyl ion is represented as $[V{\equiv}O]^{2+}$, with triple-bond status in deference to the bond order derived from the molecular orbital description (Ballhausen, C. J.; Gray, H. B. *Inorg. Chem.,* **1962**, *1*, 111) rather than the V═O representation that is commonly used], including some complexes containing sulfur-donor atoms as insulin-enhancing agents.[1−4] The application of vanadium as a potential pharmaceutical for diabetes has employed several compounds including the simple salt, $(V{\equiv}O)SO_4$, as well as pentacoordinate maltolato complexes, bis(maltolato)oxovanadium(IV) and bis(ethylmaltolato)oxovanadium(IV).[5,6] In vivo the vanadyl ion is expected to be released from the original all-oxygen-donor environment, absorbed, and transported in other forms, most likely involving serum albumin and transferrin.[4,7] The dissociation of the ligands from orally administered vanadium compounds opens up the possibility of the binding of the vanadyl ion to various biomolecules, including sulfur-containing glutathione or cysteine.

There are examples of mononuclear square-pyramidal $(V{\equiv}O)^{2+}$ complexes involving bidentate or tetradentate two-nitrogen, two-sulfur ligand sets; four have been structurally characterized by X-ray diffraction studies (Figure 1).[8−11] Structure b of Figure 1 is the bis-cysteinyl complex; the thiolate donors are trans to each other; complexes c and d, with *cis*-dithiolates, are related to the work we describe here.

Chelation through the carboxyamido nitrogen atom of the peptide backbone, although not a common coordination

*To whom correspondence should be addressed. E-mail: marcetta@mail.chem.tamu.edu.

(1) Crans, D. C.; Smee, J. J.; Gaidamauskas, E.; Yang, L. *Chem. Rev.* **2004**, *104*, 849–902 and references cited therein.
(2) Slebodnick, C.; Hamstra, B. J.; Pecoraro, V. L. *Struct. Bonding* (*Berlin*) **1997**, *89*, 51–108 and references cited therein.
(3) Monga, V.; Thompson, K. H.; Yuen, V. G.; Sharma, V.; Patrick, B. O.; McNeill, J. H.; Orvig, C. *Inorg. Chem.* **2005**, *44*, 2678–2688.
(4) Kiss, T.; Jakusch, T.; Hollender, D.; Dörnyei, A.; Enyedy, E. A.; Costa Pessoa, J.; Sakurai, H.; Sanz-Medel, A. *Coord. Chem. Rev.* **2008**, *252*, 1153–1162 and references cited therein.
(5) McNeil, J. H.; Yuen, V. G.; Hoveyda, H. R.; Orvig, C. *J. Med. Chem.* **1992**, *35*, 1489–1491.
(6) (a) Thompson, K. H.; Orvig, C. *Met. Ions Biol. Syst.* **2004**, *41*, 221–252. (b) Thompson, K. H.; Orvig, C. *Dalton Trans.* **2006**, *2006*, 761–764.
(7) Thompson, K. H.; Lichter, J.; LeBel, C.; Scaife, M. C.; McNeill, J. H.; Orvig, C. *J. Inorg. Biochem.* **2009**, *103*, 554–558.
(8) Hazari, S. K. S.; Kopf, J.; Palit, D.; Rakshit, S.; Rehder, D. *Inorg. Chim. Acta* **2009**, *362*, 1343–1347.
(9) Sakurai, H.; Taira, Z.-E.; Sakai, N. *Inorg. Chim. Acta* **1988**, *151*, 85–86.
(10) Farchione, D.; Wedd, A. G.; Tiekink, E. R. T. *Acta Crystallogr.* **1991**, *C47*, 650–651.
(11) Dutton, J. C.; Fallon, G. D.; Murray, K. S. *Inorg. Chem.* **1988**, *27*, 34–38.

Published on Web 02/07/2011

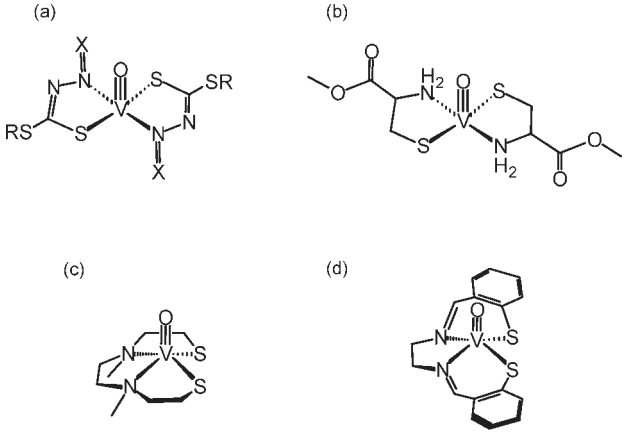

Figure 1. Examples of mononuclear square-pyramidal $V^{IV}O$ complexes containing thiolate ligation.[8−11]

mode, is observed in certain proteins and enzymes, such as serum albumin, nitrile hydratase, and acetyl coA synthase.[12−15] We have explored a series of metals bound within a dianionic N_2S_2 ligand framework utilizing diazacycles functionalized with ethylenethiolate arms, bis(mercaptoethane)-diazacyclooctane (bme-daco) and bis(mercaptoethane)-diazacycloheptane (bme-dach).[16−18] More relative to biological contiguous N_2S_2 binding sites as might be found in the tripeptide motif Cys−X−Cys is a tetraanionic N_2S_2 ligand, *N*,*N*′-ethylenebis(2-mercaptoacetamide), or ema^{4-}, which contains two aliphatic amide bonds.[19] These ligands form square-planar complexes with Ni^{II} and Cu^{II}, while ions such as Zn^{II} retain a fifth ligand and sit above the N_2S_2 plane in pseudo-square-pyramidal coordination geometry. The work herein examines the structural and spectral properties of products from the incorporation of $V{\equiv}O^{2+}$ into such dianionic and tetraanionic N_2S_2 binding sites (Chart 1). In addition, the vanadyl interaction with the Cys−Gly−Cys (CGC) peptide, the biological analogue of the tetraanionic ema^{4-} ligand, has been explored (Chart 1). Sulfur-based reactivity of the *cis*-dithiolates with the alkylating agent, 1,3-dibromopropane, is also described.

Experimental Details

Methods and Materials. All reactions were carried out using standard Schlenk techniques or in an argon-filled glovebox. Solvents were degassed and purified via a Bruker solvent system. Reagents were purchased from Aldrich Chemical Co. and used as received unless otherwise noted. The ligands *N*,*N*′-bis(2-mercaptoethyl)-1,5-diazacyclooctane (H_2-bmedaco),[20] *N*,*N*′-bis(2-mercaptoethyl)-1,5-diazacycloheptane (H_2-bmedach),[21] and *N*,*N*′-ethylenebis(2-mercaptoacetamide) (ema)[19] were prepared according to literature procedures. (Fluorenylmethoxy)-carbonyl (Fmoc)-protected amino acids (*N*-α-Fmoc-*S*-trityl-L-cysteine and *N*-α-Fmoc-glycine) and TentaGel S-RAM beads were purchased from Advanced ChemTech. Synthesis of the CGC tripeptide used standard solid-phase peptide techniques.[22]

Chart 1

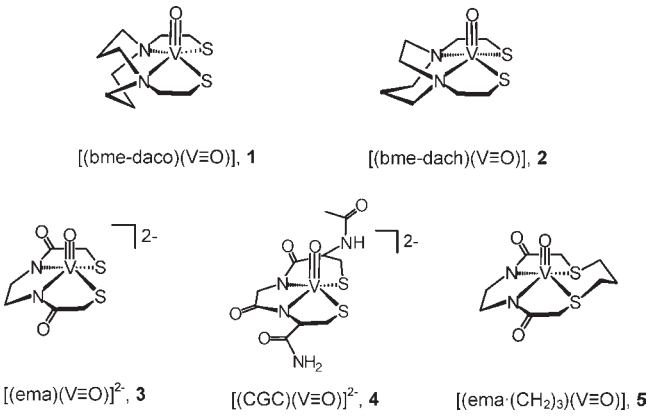

Physical Measurements. UV−vis spectra were recorded on a Hewlett-Packard 8453 diode-array spectrometer and a Cary 1E spectrophotometer using quartz cells (1.00 cm path length). IR spectra were recorded on a Bruker Tensor 37 Fourier transform IR (FTIR) spectrometer. Solution IR spectra were obtained using a CaF_2 cell with a 0.1 mm path length, and solid sample analysis was obtained using an attenuated total reflectance attachment equipped with a ZnSe crystal. Electrospray ionization mass spectrometry (ESI-MS) was performed by the Laboratory for Biological Mass Spectrometry at Texas A&M University. Elemental analyses were performed by Atlantic Microlab, Inc., Norcross, GA. EPR spectra were collected on a Bruker ESP 300 spectrometer equipped with an Oxford ER910 cryostat operating at 10 K. Samples were 1−2 mM in analyte and the spectra reported in frozen *N*,*N*-dimethylformamide (DMF) or acetonitrile solutions. The *WinEPR Simfonia* program was used to simulate the *g* and *A* parameters.[23]

X-ray Structure Analyses. Low-temperature (110 K) X-ray data were obtained on a Bruker SMART 1000 CCD-based diffractometer (Texas A&M University; molybdenum-sealed X-ray tube, Kα = 0.710 73 Å). Space groups were determined on the basis of systematic absences and intensity statistics. Structures were solved by direct methods and refined by full-matrix least squares on F^2. Hydrogen atoms were placed at idealized positions and refined with fixed isotropic displacement parameters, and anisotropic displacement parameters were employed for all non-hydrogen atoms. The following programs were used: data collection, *SMART WNT/2000*, version 5.632,[24] or *FRAMBO*, version 4.1.05 (GADDS);[25] data reduction, *SAINTPLUS*, version 6.63;[26] absorption correction, *SADABS*;[27]

(12) Darnault, C.; Volbeda, A.; Kim, E. J.; Legrand, P.; Vernede, X.; Lindahl, P. A.; Fontecilla-Camps, J. C. *Nat. Struct. Biol.* **2003**, *10*, 271–279.
(13) Margerum, D. W. *Pure Appl. Chem.* **1983**, *55*, 23 and references cited therein.
(14) Laussac, J.-P.; Sarkar, B. *Biochemistry* **1984**, *23*, 2832–2838.
(15) Nagashima, S.; Nakasako, M.; Dohmae, N.; Tsujimura, M.; Takio, K.; Odaka, M.; Yohda, M.; Kamiya, N.; Endo, I. *Nat. Struct. Biol.* **1998**, *5*, 347–351.
(16) Green, K. N.; Brothers, S. M.; Lee, B.; Darensbourg, M. Y.; Rockcliffe, D. A. *Inorg. Chem.* **2009**, *48*, 2780–2792.
(17) Almaraz, E.; Foley, W. S.; Denny, J. A.; Reibenspies, J. H.; Golden, M. L.; Darensbourg, M. Y. *Inorg. Chem.* **2009**, *48*, 5288–5295.
(18) Hess, J. L.; Conder, H. L.; Green, K. N.; Darensbourg, M. Y. *Inorg. Chem.* **2008**, *47*, 2056–2063.
(19) Kruger, H.-J.; Peng, G.; Holm, R. H. *Inorg. Chem.* **1991**, *30*, 734–742.
(20) Buonomo, R. M.; Goodman, D. C.; Musie, G.; Grapperhaus, C. A.; Maguire, M. J.; Lai, C.-H.; Hatley, M. L.; Smee, J. J.; Bellefeuille, J. A.; Darensbourg, M. Y. *Inorg. Synth.* **1998**, *32*, 89–98.
(21) Darensbourg, M. Y.; Font, I.; Pala, M.; Reibenspies, J. H. *J. Coord. Chem.* **1994**, *32*, 39–49.
(22) Krishnan, R.; Riordan, C. G. *J. Am. Chem. Soc.* **2004**, *126*, 4484–4485.
(23) *WINEPR Simfonia*, version 1.25; Bruker Analytische Messtechnik GmbH: Berlin, 1996.
(24) *SMART V5.632 Program for Data Collection on Area Detectors*; Bruker AXS Inc.: Madison, WI, 1999.
(25) *FRAMBO:FRAME Buffer Operation Version 41.05 Program for Data Collection on Area Detectors*; Bruker AXS Inc.: Madison, WI, 1999.
(26) *SAINT V6.63 Program for Reduction of Area Detector Data*; Bruker AXS Inc.: Madison, WI, 1999.
(27) Sheldrick, G. *SADABS Program for Absorption Correction Area Detector Frames*; Bruker AXS Inc.: Madison, WI, 1999.

cell refinement, *SHELXTL*;[28] structure solutions, *SHELXS-97* (Sheldrick);[29] structure refinement, *SHELXL-97* (Sheldrick).[30] The final data presentation and structure plots were generated in *X-Seed*, version 1.5.[31] Full listings of metric parameters are in the Supporting Information (SI).

***N,N′*-Bis(2-mercaptoethyl)-1,5-diazacyclooctane Oxovanadium(IV), [(bme-daco)(V≡O)], Complex 1.** The H_2-bmedaco ligand (0.84 g, 3.6 mmol) was dissolved in MeOH (30 mL), and a solution of $(acac)_2(V{\equiv}O)$ (0.87 g, 3.3 mmol) in MeOH (50 mL) was added dropwise.[32] The colorless solution immediately turned green, and upon stirring overnight, a green precipitate formed. The mixture was filtered in air; the solid was washed with 30 mL portions of Et_2O and allowed to dry in air. An analytically pure sample was obtained by recrystallization from warm CH_2Cl_2 to obtain 0.25 g (25%) of the product. Diffusion of Et_2O into a saturated solution of the complex in CH_2Cl_2 produced X-ray-quality green needlelike crystals. Elem anal. Calcd (found) for $C_{10}H_{20}N_2S_2VO$ (MW = 299 g/mol): C, 40.12 (40.12); N, 9.36 (9.25); H, 6.73 (6.55). ATR-FTIR on solid: ν(V≡O) 979 cm^{-1}. Absorption spectrum [DMF; λ_{max}, nm (ε, M^{-1} cm^{-1})]: 594 (84), 494 (119), 411 (192), 290 (2162). $^+$ESI-MS (CH_2Cl_2): *m*/*z* 300 $[(bme\text{-}daco)VO]^+$.

***N,N′*-Bis(2-mercaptoethyl)-1,5-diazacycloheptane Oxovanadium(IV), [(bme-dach)(V≡O)], Complex 2.** To a light-yellow solution of the H_2-bmedach ligand (0.785 g, 3.56 mmol) in MeOH (20 mL) was added dropwise a solution of $(acac)_2(V{\equiv}O)$ (0.951 g, 3.59 mmol) in MeOH (50 mL). The reaction mixture turned green, and a light-purple solid precipitated. The mixture was stirred at 22 °C for 20 h, and the green filtrate was separated from the purple solid. The purple solid was washed with MeOH (3 × 30 mL) and then with Et_2O (3 × 30 mL) and dried in air to afford a light-purple solid (0.75 g, 74% yield). X-ray-quality purple crystals were obtained from the slow evaporation of the green filtrate under anaerobic conditions. Elem anal. Calcd (found) for $C_9H_{18}N_2S_2VO$ (MW = 285 g/mol): C, 37.89 (37.91); N, 9.82 (9.72); H, 6.36 (6.41). ATR-FTIR on solid: ν(V≡O) 976 cm^{-1}. Absorption spectrum [DMF; λ_{max}, nm (ε, M^{-1} cm^{-1})]: 516 (118), 412 (209), 284 (2420). $^+$ESI-MS (CH_2Cl_2): *m*/*z* 286 $[(bme\text{-}dach)(VO)]^+$.

Tetraethylammonium [*N,N′*-Ethylenebis(2-mercaptoacetamide) Oxovanadium(IV)], $[Et_4N]_2$[(ema) (V≡O)], Complex 3. Under anaerobic conditions, protonated *N,N′*-ethylenebis(2-mercaptoacetamide) (0.200 g, 0.689 mmol), KOH (0.158 g, 2.82 mmol), and Et_4NCl (0.229 g, 1.382 mmol) were mixed in MeOH (30 mL) for 1 h, resulting in a light-yellow solution. A suspension of $(V{\equiv}O)(SO_4)\cdot 3H_2O$ (0.136 g, 0.627 mmol) in MeOH (35 mL) was added to the ligand mixture using a Cole-Parmer K-06417-41 plastic cannula. The reaction mixture was heated to 60−65 °C for 20 h, yielding a teal-blue solution containing a white precipitate (K_2SO_4). The solution was cooled to room temperature and filtered anaerobically, and the solvent was removed in vacuo. Acetonitrile (25 mL) was added to extract the product. Following filtration of the blue solution and several recrystallizations, x-ray-quality crystals. X-ray-quality crystals were obtained by vapor diffusion of Et_2O into the saturated MeCN solution. The blue-purple crystalline material was collected, yielding 0.225 g (68%). The product is extremely hygroscopic. Elem anal. Calcd (found) for $C_{22}H_{48}N_4S_2VO_3\cdot 2.5H_2O$ (MW = 577 g/mol): C, 37.89 (37.91); N, 9.82 (9.72); H, 6.36 (6.41). ATR-FTIR on solid: ν(V≡O) 941 cm^{-1}. Absorption spectrum [DMF; λ_{max}, nm (ε, M^{-1} cm^{-1})]: 591 (94), 387 (166), 320 (3384) nm. $^-$ESI-MS (MeCN): *m*/*z* 401 $(Et_4N)[(ema)(V{\equiv}O)]^-$.

Potassium [(Cysteinylglycylcysteinecarboxamide) Oxovandium(IV)]; K_2[(CGC)(V≡O)], Complex 4. The H_4CGC ligand (32 mg, 0.099 mmol) and KOH (11 mg, 0.196 mmol) were mixed in DMF (10 mL) and stirred for 30 min. A light-green solution of $(acac)_2(V{\equiv}O)$ (24 mg, 0.091 mmol) in DMF (15 mL) was added dropwise. The reaction was stirred for 16 h, and a light-blue-green solid was obtained after precipitation with Et_2O, yielding 28.1 mg (67% yield). ATR-FTIR on solid: ν(V≡O) 945 cm^{-1}.

[(ema)$(CH_2)_3$](V≡O)], Complex 5. To a blue solution of $[Et_4N]_2[(ema)(V{\equiv}O)]$ (0.031 g, 0.058 mmol) in MeCN (10 mL) was added neat 1,3-dibromopropane (4 μL, 0.039 mmol), resulting in a gray-blue solution within 15 min. After stirring for 30 min, the resulting solution was filtered over Celite, removing the white precipitant ($[Et_4N]Br$). The solvent was reduced in vacuo, and a reddish-blue solid was isolated. ATR-FTIR: ν(V≡O) 986 cm^{-1}. Despite repeated attempts, X-ray-quality crystals were not forthcoming.

Results and Discussion

Syntheses of Neutral [(bme-daco)(V≡O)] and [(bme-dach)(V≡O)], Complexes 1 and 2. Equation 1 describes the syntheses of complexes **1** and **2**. The neutral $N_2S_2V^{IV}{\equiv}O$ complexes are resistant to aerobic oxidation in the solid state but slowly (days) decompose in solution, presumably to yield vanadate(V) species. Complexes **1** and **2** are soluble in DMF, H_2O, and CH_2Cl_2 and slightly soluble in warm MeOH, where complex **2** was of lower solubility than **1**.

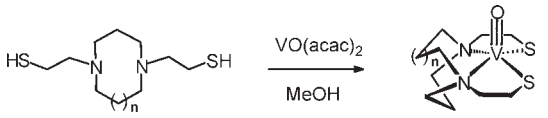

(1)

n = 1, bme-daco, **1**
n = 0, bme-dach, **2**

Dianionic $(Et_4N)_2$[(ema)(V≡O)], Complex 3. Preparation of the dianionic vanadyl complex was accomplished upon the addition of $(V{\equiv}O)SO_4$ to the deprotonated/deprotected form of the ligand in a MeOH solution with heating (60 °C), as outlined in eq 2. The tetraanionic ema ligand imparts solubility to the vanadyl-bound complex and, in addition, serves as a synthetic mimic of the N_2S_2 CGC tripeptide motif (vide infra).[33] Raymond and co-workers found that dianionic $N_2O_2(V{\equiv}O)^{2-}$ complexes containing deprotonated amide donors were stable in air in the solid state and in solution.[34] In contrast, the amide-containing dianionic $N_2S_2(V{\equiv}O)^{2-}$, complex **3**, is highly susceptible to oxidation in air both in the solid state and in solution. Exposure of MeCN solutions of complex **3** to air results in a color change from blue to red. X-ray-quality crystals obtained by the slow diffusion of Et_2O into a red MeCN solution revealed the commonly observed solution oxidation product, the decavanadate ion $V_{10}O_{28}{}^{6-}$.[1] Complex **3** was thus manipulated under air-free conditions.

(28) Sheldrick, G. *SHELXTL-PLUS, Version 4.11V, SHELXTL-PLUS Users Manual*; Siemens Analytical X-ray Instruments, Inc.: Madison, WI, 1990.
(29) Sheldrick, G. *SHELXS-97, Program for Crystal Structure Solution*; Institut fur Anorganische Chemie der Universitat Gottingen: Gottingen, Germany, 1997.
(30) Sheldrick, G. *SHELXL-97, Program for Crystal Structure Refinement*; Institut fur Anorganische Chemie der Universitat Gottingen: Gottingen, Germany, 1997.
(31) Barbour, L. J. *J. Supramol. Chem.* **2001**, *1*, 189–191.
(32) Hatley, M. L. The Vanadyl Complex of *N,N′*-bis(2-mercaptoethyl)-1,5-diazacyclooctane. M.S. Thesis, Texas A&M University, TX,1997, pp 16−18.
(33) Green, K. G.; Jeffery, S. P.; Reibenspies, J. H.; Darensbourg, M. Y. *J. Am. Chem. Soc.* **2006**, *128*, 6493–6498.
(34) Borovik, A. S.; Dewey, T. M.; Raymond, K. N. *Inorg. Chem.* **1993**, *32*, 413–421.

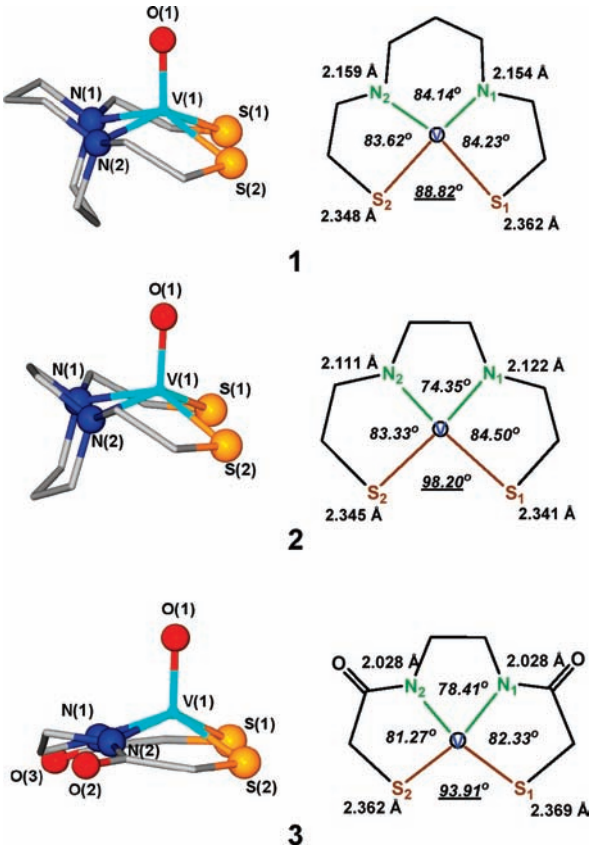

Figure 2. Ball-and-stick representations of the neutral $V^{IV}{\equiv}O$ complexes [(bme-daco)(V≡O)] (**1**) and [(bme-dach)(V≡O)] (**2**) and the dianionic $V^{IV}{\equiv}O$ complex $[Et_4N]_2$[(ema)(V≡O)] (**3**). Molecular structures are shown as thermal ellipsoids at 50% probability in the SI.

It is soluble in a wide range of solvents (H_2O, MeOH, MeCN, and CH_2Cl_2).

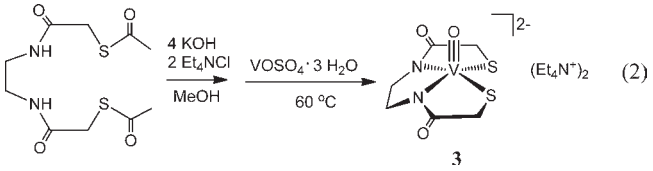

(2)

Synthesis of K_2[(CGC)(V≡O)], Complex 4. The CGC tripeptide has been complexed with Ni^{II} and Cu^{II} as metalloenzyme binding site mimics and shown to bind through deprotonated carboxyamido nitrogen atoms and thiolates, producing a tetradentate N_2S_2 coordination environment.[16,22,33] Similar to the $Ni(CGC)^{2-}$ complex, the CGC peptide derivative of vanadyl was prepared from the displacement of acac from $(acac)_2(V{\equiv}O)$ by the tripeptide in the presence of 2 equiv of KOH in a DMF solvent. A second method was accomplished by the addition of $(V{\equiv}O)SO_4$ to the deprotonated tripeptide. Both syntheses yielded light-green solids in ca. 70% yield. Comparable to its synthetic analogue **3**, complex **4** is extremely oxygen-sensitive in both the solid and solution states; the light-green color changes to red in the presence of oxygen. The dianionic vanadyl peptide complex is soluble in DMF and H_2O. The N_2S_2 coordination environment proposed for the CGC ligand bound to the vanadyl(IV) moiety is based on comparisons of its spectroscopic characterization and reactivity to the synthetic analogue complex **3**, as well as to the nickel tripeptide.[22]

Table 1. Metric Data for **1**−**3** (Distance, Å; Angle, deg)

	1	2	3
V1−O1	1.600(3)	1.605(3)	1.623(19)
V1−N1	2.154(3)	2.122(3)	2.028(2)
V1−N2	2.159(3)	2.111(3)	2.028(2)
V1−S1	2.362(17)	2.341(12)	2.369(17)
V1−S2	2.348(13)	2.346(12)	2.363(15)
N1−V1−N2	84.14(12)	74.35(11)	78.41(10)
S1−V1−S1	88.82(5)	98.20(5)	93.91(6)
N1−V1−S1	84.23(10)	84.50(8)	82.33(8)
N2−V1−S2	83.62(10)	83.34(9)	81.27(8)
N1−V1−S2	144.33(9)	141.09(9)	137.28(7)
N2−V1−S1	148.14(9)	146.39(9)	145.04(7)

Description of Molecular Structures of Complexes 1−3. Complexes **1**−**3** were characterized by X-ray diffraction analysis, and their molecular structures are presented in Figure 2; salient metric parameters are listed in Table 1. Full structural reports are given in the SI. The crystals of complex **3** exhibit pleochroism (blue/purple). In all complexes, the expected square-pyramidal coordination geometry is observed with the N_2S_2 donor set arranged around the basal plane and the vanadyl oxygen atom at the apex. The vanadium atom is displaced from the basal plane toward the apical oxygen atom by 0.6525 (**1**), 0.6521 (**2**), and 0.7125 Å (**3**). The N_2S_2 planes are quite regular with average deviations for **1** of 0.0341 Å (maximum and minimum deviations of 0.0365 Å by N2 and 0.0318 Å by S1), for **2** of 0.0481 Å (maximum and minimum deviations of 0.0561 Å by N2 and 0.0402 Å by S1), and for **3** of 0.0674 Å (maximum and minimum deviations of 0.0775 Å by N2 and 0.0572 Å by S1). The V−O bond distances are 1.600(3), 1.605(3), and 1.623(19) Å for complexes **1**−**3**, respectively. A distance ranging between 1.56 and 1.60 Å is commonly reported for the V−O distance of vanadyl complexes in square-pyramidal geometry; however, longer bond distances (> 1.60) have been observed in vanadyl complexes bound in tetraanionic ligand sets. In our series, the longer bond distance observed in complex **3** correlates with that in the IR data (vide infra).

The V−S distances are comparable to those of reported square-pyramidal vanadyl(IV) complexes and, likewise, the $V{-}N_{amine}$ and $V{-}N_{amide}$ distances are within the normal ranges.[8−11] The N−V−N angle in complex **2** is pinched by ca. 10° relative to that for the complex **1** analogue, and this constraint is compensated for by an increase in the S−V−S angle of almost 10°. Similarly, a restriction in the N−V−N angle of **3** results in an opening in the S−V−S angle also of 6° relative to **1**. A molecule of H_2O in the asymmetric unit of **3** links two adjacent complexes through hydrogen-bonding interactions to the carboxamide oxygen atoms, producing a dimer through a closed loop. To our knowledge, complex **3** represents the first example of a square-pyramidal vanadyl(IV) complex bound to *cis*-dithiolates and aliphatic diamidates in the basal plane.

The N-to-S ethylene linkers are eclipsed across the N_2S_2 planes of complexes **1**−**3**. In **1**, the metallodiazacyclohexane rings are in chair and boat configurations, with the boat opposite to the oxygen side of the vanadyl. In **2**, the single vanadium diazacyclohexane ring is in the chair confor-

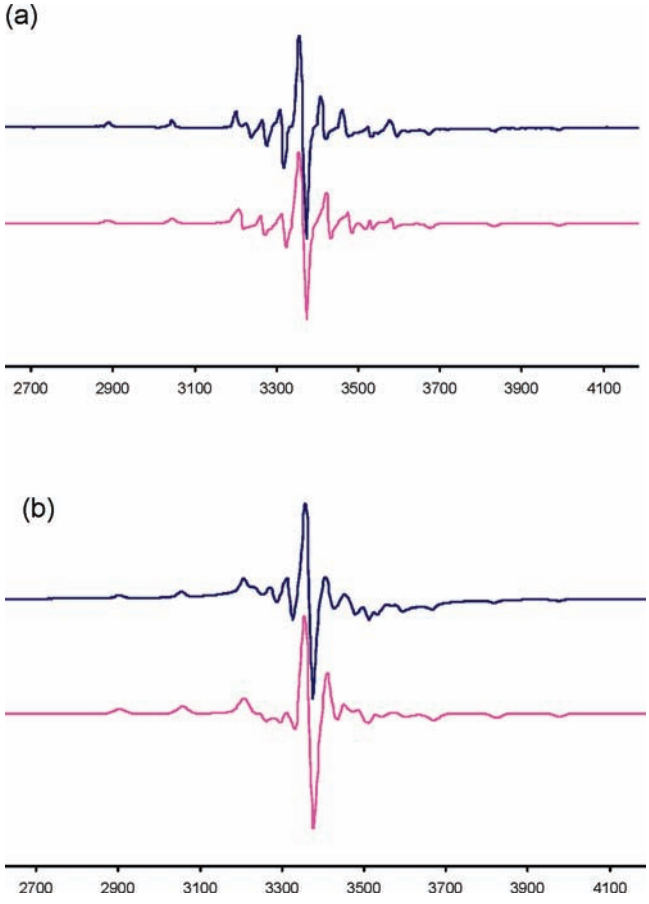

Figure 3. Frozen-solution EPR spectra of neutral $N_2S_2(V^{IV}{\equiv}O)$ complexes in DMF: (a) [(bme-daco)(V≡O)] (**1**); (b) [(bme-dach)-(V≡O)] (**2**). Top: experimental spectrum. Bottom: simulation (*WinEPR Simfonia*).

mation and opposite to the oxygen side. In this case, the two-carbon N-to-N linker is oriented toward the oxo side of the vanadyl.

IR Analysis. Complexes **1** and **2** display a ν(V≡O) band in the IR spectrum at ca. 978 cm^{-1}, which is within the typical range reported for oxovanadium complexes (935−1035 cm^{-1}).[3,35−39] The significantly lower ν(V≡O stretching frequency of **3** (941 cm^{-1}) is consistent with the longer V−O bond distance, compared to the neutral N_2S_2(V≡O) complexes. The CGC(V≡O) complex has a similarly red-shifted ν(V≡O). While the correlation of ν(V≡O) and V−O bond distances would seem to be best explained by a greater contribution of the V=O resonance form in the more electron-rich ligand fields of the tetraanionic ligand, arguments have been made that a direct relationship between the ligand field in the basal plane and the V−O bond distance cannot be made.[37] Christou et al. pointed out that dianionic complexes with electron-rich equatorial planes have V−O bond distances similar to those within neutral ligand sets (< 1.6 Å), suggesting that the V−O bond distance is influenced by factors other than the ligand charge.[37]

EPR Spectroscopy. For square-pyramidal ($V^{IV}{\equiv}O$) d^1 complexes, the unpaired electron resides in an orbital of mainly d_{xy} character, and complexes of this type exhibit spin Hamiltonian values with $g_z < g_{x,y}$ and $A_z > A_{x,y}$. The naturally occurring isotope of vanadium, ^{51}V (> 99%), with a nuclear spin of $^7/_2$, results in a signature eight-line hyperfine splitting pattern.

The frozen-solution X-band EPR spectra of the neutral $N_2S_2(V{\equiv}O)$ derivatives, complexes **1** and **2**, were recorded in DMF at 10 K (Figure 3). The spectra show the distinctive eight-line pattern expected for a d^1 vanadyl(IV) system. The EPR parameters for the (N_2S_2)-(V≡O) complexes were determined by *WinEPR Simfonia* simulation of the experimental spectra (Table 2). For comparison, Table 2 includes the EPR parameters reported for complexes with related donor sets.[3,11,38−41] Complexes **1** and **2** display larger g_x, g_y, and A_z values compared to N_2S_2 ligands containing nitrogen imine donors. The spin Hamiltonian parameters of **1** and **2** better match the values reported for O_2S_2 vanadyl complexes. In MeCN, the dianionic $(Et_4N)_2$[(ema)(V≡O)], complex **3**, displays the eight-line EPR spectra, but the signals are very broad (Figure 4). The ability of the ema^{4-} ligand to delocalize the electron density may explain the broadened lines in the spectrum of **3**. There is however a solvent effect (in DMF the spectrum considerably sharpens) that may offer another explanation. The g values of **3** are similar to those of the neutral N_2S_2 derivatives, while the A_x value is slightly larger and A_y is smaller.

The EPR spectrum of K_2[(CGC)(V≡O)], complex **4**, in DMF shows the typical hyperfine splitting and anisotropic line shapes for a $V^{IV}{\equiv}O^{2+}$ center (Figure 4). Slight differences in the EPR spectral parameters are observed between **4** and its analogue, complex **3**. The largest difference is seen in the smaller A_x and larger A_y values in **4** compared to **3**. In both **3** and **4** containing amide donors, the g values are slightly larger than those of **1** and **2** with amine donors.

Overall, a comparison of the spectroscopic properties of the crystallographically characterized **1**−**3** with those of **4** provides convincing evidence that **4** is a tetradentate analogue of **3** just as $Ni(ema)^{2-}$ and $Ni(CGC)^{2-}$ are known to be $[N_2S_2Ni]^{2-}$ analogues. The general trends in EPR parameters are higher g values and lower A values for basal-plane sulfur donors compared to their oxygen/nitrogen analogues and higher g values for dianionic complexes compared to their neutral counterparts. The most notable difference between the present complexes and others of the similar coordination environment is the larger A_z, g_x, and g_y parameters.

Reactivity of V≡O-Bound Thiolates. Extensive reactivity studies of neutral and dianionic N_2S_2M complexes with M = Ni, Zn, Cu, and Fe have established that the *cis*-dithiolate sulfur atoms may be alkylated, metalated, or oxygenated, forming stable "post-translational" sulfur-modified complexes.[16−18,42] Cornman et al. demonstrated that the reaction of a vanadate−dithiolate complex with various peroxides yielded mono- and

(35) Selbin, J. *Chem. Rev.* **1965**, *65*, 153–175.
(36) Selbin, J. *Coord. Chem. Rev.* **1966**, *1*, 293–314.
(37) Money, J. K.; Huffman, J. C.; Christou, G. *Inorg. Chem.* **1985**, *24*, 3297–3302.
(38) Klich, P. R.; Daniher, A. T.; Challen, P. R.; McConville, D. B.; Youngs, W. J. *Inorg. Chem.* **1996**, *35*, 347–356.
(39) Jezierski, A.; Raynor, J. B. *J. Chem. Soc., Dalton Trans.* **1981**, 1–7.
(40) Hanson, G. R.; Kabanos, T. A.; Keramidas, A. D.; Mentzafos, D.; Terzis, A. *Inorg. Chem.* **1992**, *31*, 2587–2594.
(41) Cornman, C. R.; Zovinka, E. P.; Boyajian, Y. D.; Geiser-Bush, K. M.; Boyle, P. D.; Singh, P. *Inorg. Chem.* **1995**, *34*, 4213–4219.
(42) Jenkins, R. M.; Singleton, M. L.; Almaraz, E.; Reibenspies, J. H.; Darensbourg, M. Y. *Inorg. Chem.* **2009**, *48*, 7280–7293.

Table 2. EPR Parameters for Oxovanadium(IV) Complexes[a]

complex	donor set	g_z	g_x	g_y	A_z	A_x	A_y
[(bme-daco)(V≡O)], **1**	N_2S_2	1.968	1.991	1.9945	157.40	52.60	42.95
[(bme-dach)(V≡O)], **2**	N_2S_2	1.967	1.9915	1.995	153.27	53.67	38
$(Et_4N)_2$[(V≡O)(ema)], **3**	N_2S_2	1.970	2.001	2.001	153.27	60	33
$(K)_2$[(CGC)(V≡O)], **4**	N_2S_2	1.9695	1.999	1.999	156.41	51.60	42
[(ema)(V≡O)·$(CH_2)_3$], **5**[b]	N_2S_2	1.977	2.000	2.000	153.12	49	33
VO(tsalen)[c]	N_2S_2	1.978	1.986	1.986	148	51	51
[VO(tsatln)][c]	N_2S_2	1.966	1.975	1.975	140	37	37
[VO(tsalphen)][c]	N_2S_2	1.967	1.987	1.987	145	51	51
$[VO(mp)_2]^{2-}$ [d,e]	O_2S_2	1.975	2.007	1.999	150	40	40
$[VO(mmppt)]_2$ [f,g]	O_2S_2	1.958	1.985	1.981	151	42	52
[VO(salen)][h]	N_2O_2	1.955	1.986	1.989	166	56	55
[VO(pycac)][i,j]	N_3O	1.9558	1.9777	1.9811	151.43	53.29	42.46
VO(PAIS)[k,l]	N_3O	1.961	1.986	1.982	154	45	54

[a] In frozen DMF. [b] In frozen MeCN. [c] Reference 1111. [d] Measured in frozen CH_2Cl_2/DMF. [e] Reference 38. [f] Measured in frozen CH_2Cl_2/DMF. [g] Reference 3. [h] Reference 39. [i] Reference 40. [j] Measured in chloroform at 120 K. [k] Measured in frozen DMF/EtOH. [l] Reference 41.

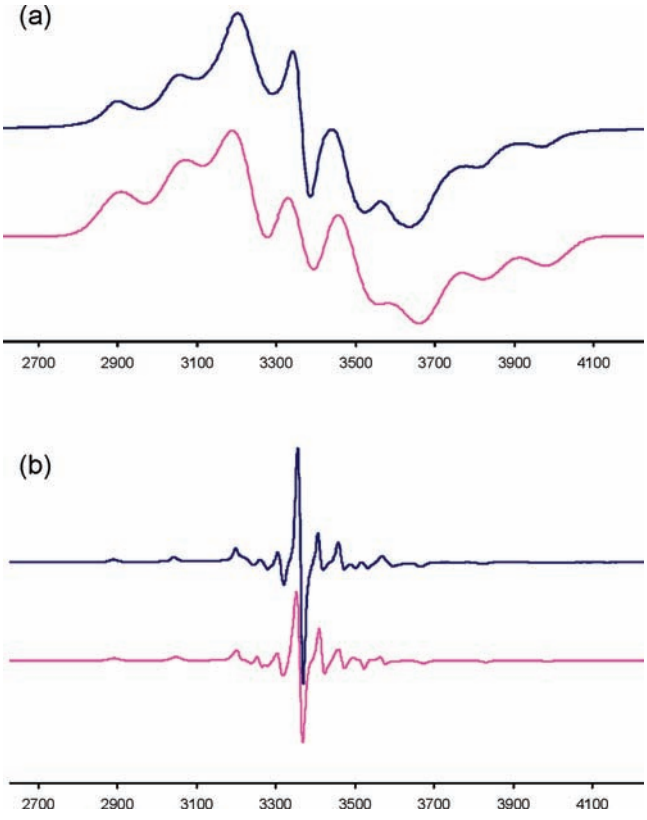

Figure 4. Frozen-solution EPR spectra of dianionic $N_2S_2(V^{IV}≡O)$ complexes: (a) $(Et_4N)_2$[(ema)(V≡O)] in MeCN, **3**; (b) $(K)_2$[(CGC)(V≡O)] in DMF, **4**. Top: experimental spectrum. Bottom: simulation (*WinEPR Simfonia*).

disulfenate complexes.[43] The incorporation of the vanadyl ion in the N_2S_2-donor environments described above permits examination of the nucleophilicity of *cis*-dithiolates when bound to vanadyl(IV).

The reaction of neutral $N_2S_2(V≡O)$ complexes **1** and **2** with 1,3-dibromopropane did not lead to S-alkylated products, even under reflux conditions. This result contrasts with the reaction of (bme-daco)Ni or (bme-dach)Ni, which readily forms macrocyclic $[(N_2S_2)Ni]^{2+}$ complexes. However, as represented in Scheme 1, the addition of neat 1,3-dibromopropane to a blue MeCN solution of

(43) Cornman, C. R.; Stauffer, T. C.; Boyle, P. D. *J. Am. Chem. Soc.* **1997**, *119*, 5986–5987.

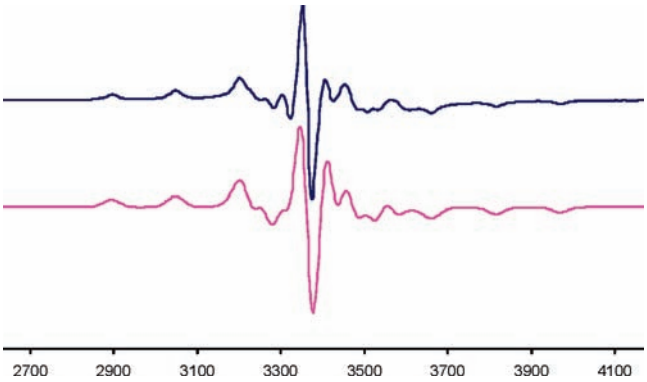

Figure 5. Frozen-solution EPR spectra of neutral complex [(ema)·$(CH_2)_3$(V≡O)] (**5**) in MeCN. Top: experimental spectrum. Bottom: computer-simulated spectrum.

Scheme 1

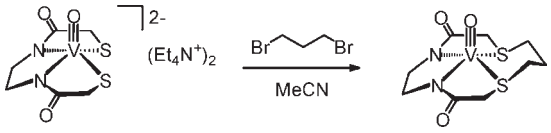

complex **3**, $VO(ema)^{2-}$, results in the formation of a white precipitate of Et_4NBr and a grayish-blue solution within 15 min. Neutral complex **5**, [(ema)$(CH_2)_3$(V≡O)], was isolated as a reddish-blue solid; however, efforts to obtain crystals have been unsuccessful. Solubility in CH_3CN, CH_2Cl_2, and DMF indicates a neutral complex. The ν(V≡O) frequency in the ATR-FTIR spectrum displays a band at 986 cm^{-1}, which is shifted positively by 41 cm^{-1} compared to the dianionic vanadyl precursor, complex **3**. This is as expected for a decrease of the electron density in the basal plane. The EPR spectrum of [(ema)·$(CH_2)_3$(V≡O)] in frozen MeCN (Figure 5) differs from that of the precursor, in that the broad features of dianionic **3** resolve into distinctive sharp hyperfine lines. The g_z value increases, and the A_x parameter decreases.

Conclusions

The synthesis and characterization of five $N_2S_2(V^{IV}≡O)$ complexes that incorporate either amine/thiolate, amide/thiolate, or amide/thioether donor sets have been described. The neutral $N_2S_2(V^{IV}≡O)$ species show stability to aerobic oxidation in the solid state, while the $[N_2S_2(V^{IV}≡O)]^{2-}$ complexes are oxygen-sensitive, leading ultimately to

oxovanadium(V) clusters; intermediate *S*-oxygenates have not yet been observed. The products of oxygen-atom addition to the former neutral complexes using more reactive oxygen species are under investigation. The product(s) of aerobic oxidation have not been defined; however, in one case, the amide donors in previously reported $V^{IV}{\equiv}O$ complexes are linked to aromatic backbones, whereas the amido nitrogen donors presented herein extend from aliphatic chains, better mimicking peptide binding sites. Three of the complexes, **1**−**3**, were structurally characterized by X-ray diffraction analysis. In each case, the complexes are five-coordinate with square-pyramidal geometry, and the V≡O moiety is significantly (0.65−0.71 Å) displaced from the basal plane. The suggested structure for the product of the $V{\equiv}O^{2+}$ ion bound to the deprotonated peptide, CGC^{4-}, is based on (1) the presence of a strong IR band at 940 cm^{-1}, indicative of a V≡O group, and (2) EPR parameters that parallel the complexes within this N_2S_2 series. Although dianionic $[O_2S_2(V^{IV}{\equiv}O)]^{2-}$ complexes have been shown to display similar V≡O stretching frequencies, the EPR parameters for the $[(CGC)(V{\equiv}O)]^{2-}$ complex more closely resemble those from $V{\equiv}O^{2+}$ in a $[N_2S_2]^{4-}$ ligand field.[44] From these similar spectroscopic results, we conclude that the vanadyl ion is bound in N_2S_2 coordination within the CGC peptide. This is consistent with the known N_2S_2 binding of CGC to Cu^{2+} and Ni^{2+}.[16,33]

The EPR spectra indicate the presence of paramagnetic $V^{IV}{\equiv}O$ species in all of the complexes presented herein, and the EPR parameters (g values of 1.91−2.0) are indicative of strong σ donation from the basal-plane ligands.[34] The replacement of the amine donors with amides results in slightly higher g_x and g_y values, which suggests a slight increase in σ donation in the basal plane. Notably, in CH_3CN complex **3** displays very broad signals in its EPR spectrum. The absence of sharp hyperfine splitting in complex **3** may be due to delocalization of the unpaired electron over the ligand and metal, thus reducing the unpaired electron coupling with the vanadium nucleus. However, a solvent effect cannot be ruled out. Upon neutralization of the charge as in the S-alkylated complex **5**, sharp hyperfine signals return to the EPR spectrum. In this regard, a previous natural bond orbital (NBO) analysis and electrostatic potential maps of the Ni^{2+} analogues of complexes **3** and **5** indicated that the electron density in the dianionic $[Ni(ema)]^{2-}$ complex is substantially delocalized and largely on the thiolate sulfur lone pairs and amido nitrogen lone pairs, with covalent bond character in the Ni−S bond and dative bond character in the Ni−N bond.[16] The NBO analysis of the $[Ni(ema)]\cdot(CH_2)_3$ complex derived from alkylation showed that the electron distribution becomes localized on the amido nitrogen atoms, resulting in the reverse: Ni−S dative bond character and Ni−N covalent character.[16] It would appear that the same is happening in the vanadyl case.

The significantly lower V≡O stretching frequencies observed for the dianionic complexes, **3** and **4**, may be a result of the increase in the electron richness about the $V^{IV}{\equiv}O$ center compared to neutral complexes **1** and **2**. Consistently, upon alkylation of **3** to yield **5**, the ν(V≡O) band shifts positively to 986 cm^{-1}. Together, these results support our hypothesis that the electronic distribution of complex **3** is delocalized, which, in turn, affects the interaction of the unpaired electron with the vanadium nucleus.

In contrast to neutral N_2S_2Ni complexes, which readily react with a range of electrophiles, there was no evidence of reactivity of the thiolates in the neutral $N_2S_2(V^{IV}{\equiv}O)$ complexes. However, along with the alkylation reactions described above, preliminary studies find that only the dianionic complexes **3** and **4** readily form $W(CO)_5$ and $W(CO)_4$ adducts. The biological relevance of thiolates and amide binding in proteins was noted in the Introduction. This work adds to the chemistry of oxovanadium binding to *N*-amides, which are naturally occurring in peptides and *S*-thiolates, demonstrating that stable $V^{IV}{\equiv}O$ complexes can be formed with binding sites that consist of such donors.

Acknowledgment. We gratefully acknowledge financial support from the National Science Foundation (Grant CHE-0910679) and the Robert A. Welch Foundation (Grant A-0924).

Supporting Information Available: X-ray crystallographic files in CIF format for the structure determination of complexes **1**−**3** and tables of crystal data and full listing of metric parameters for those compounds. This material is available free of charge via the Internet at http://pubs.acs.org.

Note Added after ASAP Publication. This paper was published on the Web on February 7, 2011. Additional minor text changes were made and equation 2 was revised. The corrected version was reposted on February 10, 2011.

(44) Klich, P. R.; Daniher, A. T.; Challen, P. R.; McConville, D. B.; Youngs, W. J. *Inorg. Chem.* **1996**, *35*, 347–356.